AIP | Applied Physics Letters

Effect of film thickness and biaxial strain on the curie temperature of EuO

A. Melville, T. Mairoser, A. Schmehl, T. Birol, T. Heeg et al.

Citation: Appl. Phys. Lett. **102**, 062404 (2013); doi: 10.1063/1.4789972
View online: http://dx.doi.org/10.1063/1.4789972
View Table of Contents: http://apl.aip.org/resource/1/APPLAB/v102/i6
Published by the American Institute of Physics.

Effect of film thickness and biaxial strain on the curie temperature of EuO

A. Melville,[1] T. Mairoser,[2] A. Schmehl,[2] T. Birol,[3] T. Heeg,[4] B. Holländer,[4] J. Schubert,[4] C. J. Fennie,[3] and D. G. Schlom[1,5]
[1]*Department of Materials Science and Engineering, Cornell University, Ithaca, New York 14853, USA*
[2]*Zentrum für elektronische Korrelationen und Magnetismus, Universität Augsburg, Universitätsstraße 1, 86159 Augsburg, Germany*
[3]*School of Applied and Engineering Physics, Cornell University, Ithaca, New York 14853, USA*
[4]*Peter Grünberg Institute, PGI 9-IT, JARA-FIT, Research Centre Jülich, D-52425 Jülich, Germany*
[5]*Kavli Institute at Cornell for Nanoscale Science, Ithaca, New York 14853, USA*

(Received 24 September 2012; accepted 4 January 2013; published online 11 February 2013)

The effects of film thickness and epitaxial strain on the magnetic properties of commensurate EuO thin films grown on single crystalline (001) yttria-stabilized zirconia (YSZ) and (110) $LuAlO_3$ substrates are presented. Magnetic measurements show a reduction in the Curie temperature (T_C) for EuO/YSZ films thinner than ~10 nm. Additionally, the EuO/$LuAlO_3$ films exhibit a systematically lower T_C than the corresponding EuO/YSZ films. This further reduction in T_C is attributed to the effect of biaxial tensile strain arising from lattice mismatch: 0.0% for EuO/YSZ and +1.0% for EuO/$LuAlO_3$. © *2013 American Institute of Physics*. [http://dx.doi.org/10.1063/1.4789972]

Europium oxide (EuO) has a rocksalt structure ($a = 5.144$)[1] with Eu^{2+} cations whose half-filled 4*f* orbital is responsible for a large ferromagnetic response below its Curie temperature (T_C) of 69 K.[2] This pronounced ferromagnetism induces a metal-to-insulator transition spanning up to 13 orders of magnitude in resistivity[3] and spin-polarization of 96%,[4] as a result of conduction band splitting by 0.6 eV.[5,6] This makes EuO exceptional and of interest for spintronic applications.

The low bulk T_C restricts the utilization of EuO in device applications, so overcoming this limitation is one of the key challenges yet to be addressed. Theoretical predictions indicate that the T_C can be manipulated by injecting electrons into the system[7] or by straining the crystal.[8] The added electrons enhance the T_C by filling the spin-polarized conduction band, thus adding to the magnetic exchange energy of the system. In fact, doping with 3^+ cations like lanthanum,[9–11] gadolinium,[9,12–15] or oxygen vacancies[3,9,16–18] is a common technique for injecting electrons, increasing the T_C up to a maximum reported value of 200 K.[11,19] The strain-induced T_C manipulation is driven by altering the distance between the magnetic 4*f* electrons relative to the bulk spacing. Increasing this distance leads to a reduced T_C, while reducing this distance causes an enhanced T_C. In thin films biaxial strain can be achieved via commensurate, epitaxial growth to a well-chosen substrate with a specific lattice mismatch.

In this letter we contrast the dependence of the magnetic properties on thickness in a series of strain-free epitaxial EuO films with that of +1% biaxially strained epitaxial EuO films to determine the effect of strain on T_C. The unstrained films were grown on (001) 9.5 mol % yttria-stabilized cubic zirconia (YSZ). YSZ is nearly lattice-matched to EuO with a lattice constant of 5.140 Å.[20] The epitaxial orientation relationship is cube-on-cube with (001) EuO ∥ (001) YSZ and [100] EuO ∥ [100] YSZ. For comparison, strained EuO films were grown on (110) $LuAlO_3$. $LuAlO_3$ is an orthorhombic perovskite similar to $YAlO_3$, and the (110) surface has a rectangular surface net with in-plane lattice constants of 7.379 Å along the [1$\bar{1}$0] direction and 7.300 Å along the [001] direction.[21] The expected epitaxial orientation relationship is (001) EuO ∥ (110) $LuAlO_3$ with [1$\bar{1}$0] EuO ∥ [001] $LuAlO_3$ and [110] EuO ∥ [110] $LuAlO_3$, with a linear lattice mismatch of +0.4% and +1.5% along the EuO [1$\bar{1}$0] and [110] directions, respectively.

All films were grown in a Veeco Gen10 molecular-beam epitaxy chamber with a chamber background pressure of $\sim 2 \times 10^{-9}$ Torr. The EuO films on YSZ were grown at a substrate temperature of 400 °C after annealing the substrates at 650 °C in an oxygen background partial pressure of 3×10^{-7} Torr prior to growth to form a well-ordered surface.[22] For films thicker than 10 nm, the EuO films on $LuAlO_3$ were grown at 550 °C.[23] For films thinner than 10 nm, the EuO films on $LuAlO_3$ were grown at 400 °C, to match the growth conditions to the films grown on YSZ. All films were grown within an adsorption-controlled growth regime.[23] During the growth, oxygen was introduced yielding a chamber background pressure of less than 1×10^{-8} Torr. The incident flux of europium atoms was calibrated to 1.1×10^{14} atoms/(cm^2·s) using a quartz crystal microbalance, approximately 20% higher than the EuO growth rate, which had been determined earlier from areal density measurements of the europium content of calibration samples using Rutherford backscattering spectrometry (RBS). Growth under europium-excess conditions is key to the adsorption-controlled deposition of EuO. The samples were capped with 30 nm of amorphous silicon or 100 nm of aluminum immediately after the growth to prevent further oxidation during *ex situ* characterization. A series of films with thicknesses varying from 1.5 nm to 170 nm (as measured by RBS) were grown both on YSZ and on $LuAlO_3$ substrates. Structural measurements were made using a four-circle X-ray diffractometer (XRD) equipped with Cu K_α radiation. Magnetic measurements were performed using superconducting quantum interference device (SQUID) magnetometry. SQUID measurements to determine T_C were made in zero applied field for all samples.[38]

The θ–2θ scan of a 40 nm thick EuO film grown on YSZ (Fig. 1(a)) exhibits only peaks at $2\theta = 34.9°$ and 73.8°,

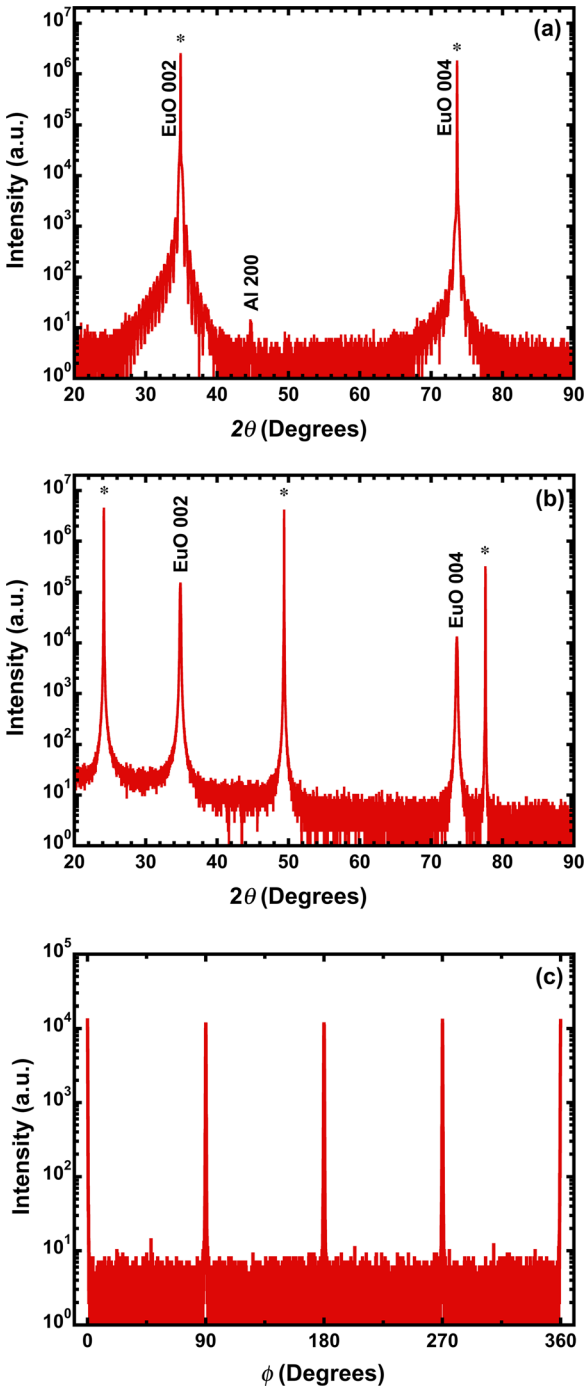

FIG. 1. θ–2θ scans of (a) 40 nm thick EuO/YSZ and (b) 170 nm thick EuO/$LuAlO_3$ films. Both scans reveal phase-pure EuO with no indication of Eu metal, Eu_3O_4, or Eu_2O_3 and are characteristic of all EuO films grown in this study. (c) ϕ-scan of 111 EuO diffraction peaks of the same film studied in (b) at $\chi = 35.3°$ showing the epitaxial relationship of EuO on $LuAlO_3$ to be $[1\bar{1}0](001)$ EuO ∥ [001](110) $LuAlO_3$. $\chi = 90°$ aligns the diffraction vector perpendicular to the plane of the substrate. $\phi = 45°$ is aligned to be parallel to the [001] in-plane direction of the (110) $LuAlO_3$ substrate (Ref. 37).

consistent with the growth of phase-pure epitaxial EuO. The complete overlap of film and substrate peaks occurs because EuO and YSZ both have face-centered cubic lattices with nearly identical parameters ($a_{YSZ} = 5.140$ Å[20] and $a_{EuO} = 5.144$ Å[1]). These features were observed for all EuO/YSZ films. The θ–2θ scan of a 170 nm thick EuO/$LuAlO_3$ film is shown in Fig. 1(b) and reveals only substrate peaks and 00ℓ EuO peaks, as did all EuO/$LuAlO_3$ films included in this study, indicating that these samples are also phase-pure within the resolution of our XRD measurements. Figure 1(c) shows a ϕ-scan of the 111 off-axis EuO peaks of the same film studied in Fig. 1(b), which, together with the θ–2θ scan, confirm the epitaxy of EuO on $LuAlO_3$ with an orientation relationship of [110] (001) EuO ∥ $[1\bar{1}0]$ (110) $LuAlO_3$.

The interplanar spacings of the (110) and $(1\bar{1}0)$ planes of a strained EuO film were calculated from the measured θ–2θ positions of multiple reflections from the (001), (111), and $(1\bar{1}1)$ planes of a 10 nm thick film. The lattice spacing along [110] EuO was 3.694 ± 0.005 Å and the lattice spacing along $[1\bar{1}0]$ EuO was 3.652 ± 0.005 Å, which match the $d_{2\bar{2}0}$ and d_{002} interplanar spacings of the $LuAlO_3$ substrate within experimental error. The out-of-plane spacing was 5.123 ± 0.005 Å, which agrees with the expected value (5.122 Å) based on the biaxial strain and the elastic constants of EuO.[24] These results indicate that the EuO films up to 10 nm in thickness are commensurately strained to the underlying substrate.

Rocking curves of the 002 EuO diffraction peak were taken by rocking the substrate along its $[1\bar{1}0]$ and [001] axes because the film strain is different from these two substrate directions. In Fig. 2, the full width at half maximum (FWHM) of the EuO films along these directions is plotted as a function of film thickness. The FWHM of the substrates ranged from 25 to 37 arc sec. The FWHM for the thin films was as low as 38 arc sec, with a dramatic increase in FWHM for films thicker than 69 nm. This broadening of the rocking curve is attributed to film relaxation via the introduction of stress-reducing defects, e.g., dislocations.[25–27] The critical thickness for the onset of observable relaxation in epitaxial EuO on (110) $LuAlO_3$ using our growth conditions is thus 69 ± 5 nm. This is nearly twice the critical thickness reported for EuO films grown commensurately under similar growth conditions on (110) $YAlO_3$ (38 nm),[23] which has an average lattice mismatch that is nearly twice that of $LuAlO_3$ (+1.8%). Additionally, the onset of relaxation for EuO/$LuAlO_3$ is the same along both the $[1\bar{1}0]$ and [001] in-plane directions of the substrate, despite a difference in in-plane strain of more than 1%. This indicates that the relaxation mechanism for the two directions is coupled.

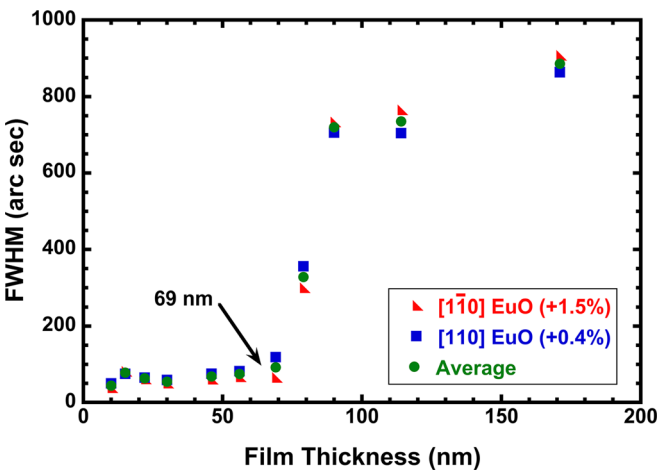

FIG. 2. The FWHM of the EuO 002 rocking curves made by rocking about both the [110] high strain (red triangles) and $[1\bar{1}0]$ low strain (blue squares) substrate axes plotted as a function of thickness of the EuO/$LuAlO_3$ films. The average FWHM (green circles) is also plotted. The arrow indicates the critical thickness for distinguishable relaxation, 69 ± 5 nm.

Figure 3 compares the Curie temperatures of these epitaxial EuO films as a function of thickness on both YSZ and $LuAlO_3$ substrates. The YSZ series explores the effect of film thickness in unstrained epitaxial EuO. The T_C is reduced below a film thickness of ~10 nm, which is expected because of too few neighboring magnetic atoms[28,29] and consistent with other reports that describe a reduced T_C below a thickness of 4–10 nm in polycrystalline EuO films.[29–31] Furthermore, the reduction in T_C matches both the predictions of the theory by Schiller *et al.*[28] and mean-field approximation considering nearest neighbors and next-nearest neighbors for films thicker than 5 nm.[29,31] These calculations are plotted alongside the data in Fig. 3.

To predict the effect of biaxial strain on the T_C of an epitaxial (001) EuO film commensurately grown on a (110) $LuAlO_3$ substrate, we performed first principles calculations using density functional theory (DFT) as implemented in VASP.[32] The generalized gradient approximation[33] together with an on-site Coulomb energy (GGA+U) formalism was used in order to better take into account the localized nature of the *f* electrons. An external pressure was applied during the relaxation of the crystal structure in order to correct for the overestimation of volume by GGA. The pressure required was determined by calculations for bulk EuO with cubic symmetry. The pressure value obtained from these calculations was applied during subsequent calculations in which biaxial strain was imposed on the EuO and its in-plane lattice constants were kept fixed, but the out-of-plane one was allowed to relax.

Our calculations cover the biaxial strain range ±2.0%, since EuO is predicted to undergo a structural phase transition at large values of biaxial strain, which is beyond the scope of this work.[34] We confirmed the absence of a structural phase transition within our strain range by calculating the frequencies of both the zone center and the zone boundary phonon modes. Furthermore, high pressure (and with it the corresponding change in lattice parameter) leads to a fluctuating electron configuration between $4f^7 5d^0$ and $4f^6 5d^1$ in EuO and causes a downturn in T_C above 14 GPa.[35,36] The details of such dynamic fluctuations are beyond the reach of standard DFT+U calculations. The strain range we consider, however, is sufficiently far from both electron configuration and structural transitions such that our calculations should predict the correct trend of T_C.

In order to calculate the exchange constants precisely, we built 32 atom supercells for each biaxial strain value and fit energies of 8 different spin configurations to an Ising model. Calculations for cubic EuO indicated that 3rd and 4th nearest neighbor exchange couplings are negligible, so we ignored them in our calculations of EuO under biaxial strain. In order to get an estimate of T_C, we used a mean-field model. As expected from DFT and mean field approximations, T_C is grossly overestimated by our calculations; further, T_C depends on the exact value of U chosen. As we are interested in the change in T_C with strain, in Fig. 4 we present T_C/T_{C0}, i.e., the ratio of the Curie temperature under biaxial strain to that in bulk. The calculations were performed for a range of reasonable U values, the results of which are denoted with different colors and shapes in Fig. 4. The calculated change in T_C for different U overlap well, indicating that the result is robust and physically meaningful. T_C decreases with increasing biaxial strain, which is consistent with Ref. 8.

In order to explore the effect of the anisotropic strain induced by the (110) $LuAlO_3$ substrate (+0.4% and +1.5% along perpendicular in-plane directions in a commensurate (001) EuO film), we also calculated the exchange constants and the resultant T_C for the anisotropic boundary conditions corresponding specifically to $LuAlO_3$. The ratio of the resultant Curie temperature to that of bulk is presented as the squares at 0.95% strain in Fig. 4. The fact that these squares lie in-line with other points, all calculated with isotropic

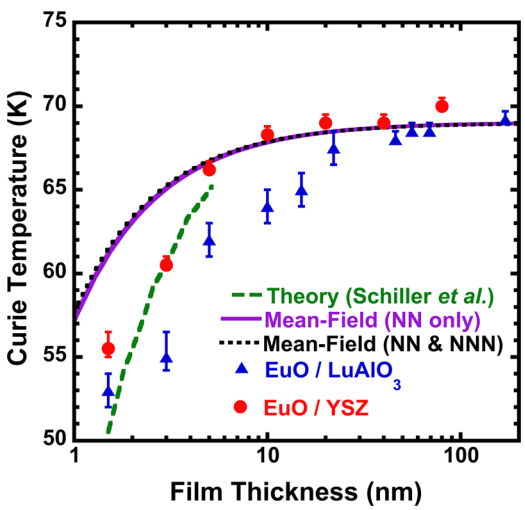

FIG. 3. The Curie temperature as a function of film thickness is compared for EuO/YSZ (red circles) and EuO/$LuAlO_3$ (blue triangles). The T_C is reduced below the bulk T_C of 69 K for films thinner than 10 nm for EuO/YSZ as a result of size effects. The T_C of EuO/$LuAlO_3$ is lower than the T_C of EuO/YSZ for films below the critical thickness for relaxation on $LuAlO_3$, about 69 nm. Films thicker than this exhibit a T_C that asymptotes to the bulk T_C of unstrained EuO (69 K). The theory presented by Schiller *et al.* (Ref. 28) is displayed by the dashed green line; the mean-field approximation considering only nearest neighbors (NN) is displayed by the solid purple line (Ref. 31), and the mean-field approximation considering both nearest neighbors and next-nearest neighbors (NNN) is displayed by the dotted black line (Ref. 29).

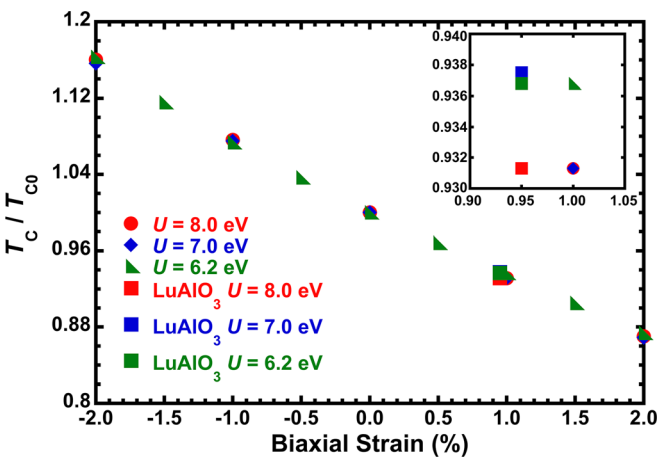

FIG. 4. Calculated effect of biaxial strain on the T_C of EuO. The effect of changing the on-site Coulomb energy U in the density functional theory on the resulting T_C is shown by the colored data points. The squares represent the specific case of the biaxial strain imparted by a (110) $LuAlO_3$ substrate on a commensurate epitaxial (001) EuO film. The inset shows that the reduction in T_C for EuO films grown commensurately on $LuAlO_3$ is ~6%.

in-plane biaxial strain, indicates that the anisotropy of the substrate surface does not lead to an important difference and that T_C is decreased by the same amount as it would be on a substrate with an isotropic surface and the same average lattice constant. The calculated decrease in T_C for commensurate (001) EuO on (110) $LuAlO_3$ is about 6%, which corresponds to ~4 K with respect to bulk. We emphasize that our standard DFT calculations utilize periodic boundary conditions, corresponding to a film that is infinite in all dimensions, such that finite-size effects are not considered.

These calculations match, within the error bars, the T_C of the commensurate EuO/$LuAlO_3$ films that are unaffected by finite-size effects, that is, films thicker than 10 nm. Furthermore, the T_C of all commensurate EuO/$LuAlO_3$ films are consistently reduced relative to the T_C of the EuO/YSZ films. For example, a 1.5 nm EuO film on YSZ has a T_C of 56 ± 1 K, while a 1.5 nm EuO film on $LuAlO_3$ has a T_C of 53 ± 1 K. EuO/$LuAlO_3$ films thicker than 69 nm are partially relaxed and as the strain diminishes, the T_C recovers to that of bulk EuO (69 K). As the only difference between these films is the strain imparted by epitaxial misfit from the different substrates, the T_C reduction is attributed to the imposed biaxial tensile strain, which is in agreement with our calculations and the literature.[8]

Figure 5(a) shows the onset of magnetization for a fully commensurate EuO film (10 nm thick) and a fully relaxed EuO film (170 nm thick) on $LuAlO_3$. The T_C of the 10 nm thick film was 64 ± 1 K, and the T_C of the 170 nm thick film was 69 ± 1 K. This matches, within the error, the DFT calculations, which predict a 6% decrease in the T_C for the case of EuO/$LuAlO_3$. Figure 5(b) compares the magnetic hysteresis in the same films. The coercive field of the 10 nm thick sample was 55 ± 10 G, and the coercive field of the 170 nm thick sample was 47 ± 10 G. The saturation magnetization was $5.5 \pm 0.2\ \mu_B$ per europium atom for the 10 nm thick film and $6.6 \pm 0.2\ \mu_B$ per europium atom for the 170 nm thick film. These are both close to the theoretical maximum of 7 μ_B per europium atom and other reports of EuO thin films.[10,13,23] Though the effect of strain on the coercive field and saturation magnetization is likely non-zero, it is not significant and could not be determined in our experiment.

In conclusion EuO is shown to grow epitaxially on (110) $LuAlO_3$ substrates with an epitaxial orientation relationship of [110](001) EuO ‖ [1$\bar{1}$0](110) $LuAlO_3$ and is commensurate below a critical thickness of 69 nm. The T_C of EuO/YSZ, which shows size effects for films thinner than 10 nm, was compared to the T_C of EuO/$LuAlO_3$. By comparing the T_C vs. thickness of unstrained EuO/YSZ with strained EuO/$LuAlO_3$, a reduction in T_C caused by the biaxial tensile strain is clearly observed, in addition to the reduction in T_C from size effects.

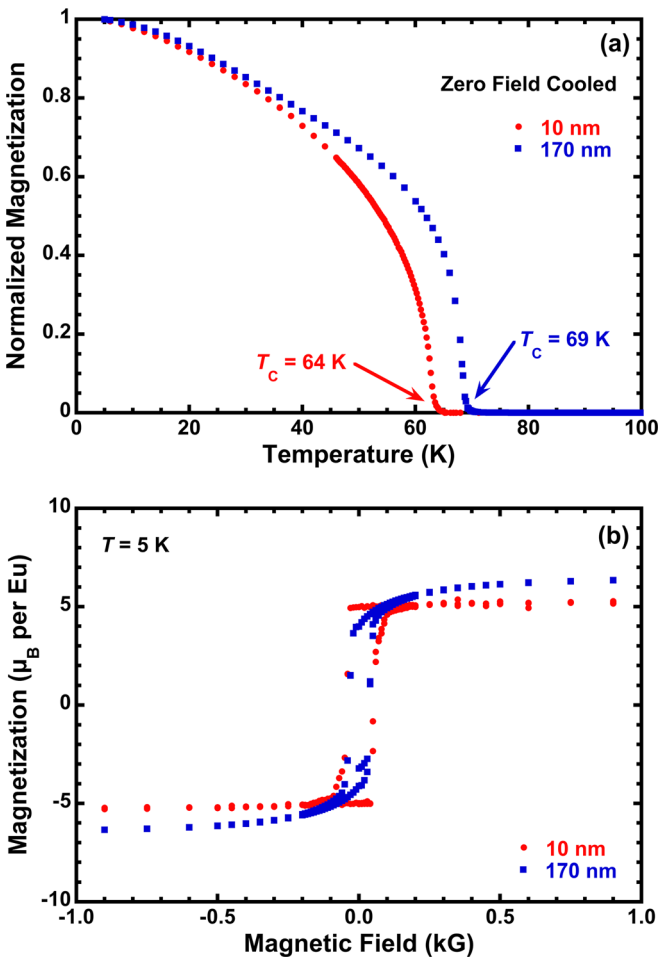

FIG. 5. (a) Magnetization as a function of temperature measurements indicate a clear onset of magnetization in the absence of an applied magnetic field (Ref. 38) at 64 K in the 10 nm thick film and 69 K in the 170 nm thick film. (b) Magnetic hysteresis curves for the 10 nm and 170 nm thick EuO thin films.

The work at Cornell was supported by the AFOSR (Grant No. FA9550-10-1-0123). The work in Augsburg was supported by the DFG (Grant No. TRR 80). A.M. gratefully acknowledges support from the NSF IGERT Program (NSF Award No. DGE-0654193) and by the IMI Program of the National Science Foundation under Award No. DMR 0843934. T.B. and C.J.F. were supported by the DOE-BES # DE-SC0002334.

[1]H. A. Eick, N. C. Baenziger, and L. Eyring, J. Am. Chem. Soc. **78**, 5147–5149 (1956).
[2]T. R. McGuire and M. W. Shafer, J. Appl. Phys. **35**, 984–988 (1964).
[3]G. Petrich, S. Von Molnár, and T. Penney, Phys. Rev. Lett. **26**, 885–888 (1971).
[4]A. Melville, T. Mairoser, A. Schmehl, D. E. Shai, E. J. Monkman, J. W. Harter, T. Heeg, B. Holländer, J. Schubert, K. M. Shen, J. Mannhart, and D. G. Schlom, Appl. Phys. Lett. **100**, 222101 (2012).
[5]S. Von Molnár, IBM J. Res. Dev. **14**, 269–275 (1970).
[6]P. G. Steeneken, L. H. Tjeng, I. Elfimov, G. A. Sawatzky, G. Ghiringhelli, N. B. Brookes, and D.-J. Huang, Phys. Rev. Lett. **88**, 047201 (2002).
[7]S. Methfessel, Z. Angew. Phys. **18**, 414–432 (1965).
[8]N. J. C. Ingle and I. S. Elfimov, Phys. Rev. B **77**, 121202 (2008).
[9]M. W. Shafer and T. R. McGuire, J. Appl. Phys. **39**, 588–590 (1968).
[10]A. Schmehl, V. Vaithyanathan, A. Herrnberger, S. Thiel, C. Richter, M. Liberati, T. Heeg, M. Röckerath, L. F. Kourkoutis, S. Mühlbauer, P. Böni, D. A. Muller, Y. Barash, J. Schubert, Y. Idzerda, J. Mannhart, and D. G. Schlom, Nat. Mater. **6**, 882–887 (2007).
[11]H. Miyazaki, H. J. Im, K. Terashima, S. Yagi, M. Kato, K. Soda, T. Ito, and S. Kimura, Appl. Phys. Lett. **96**, 232503 (2010).
[12]H. Ott, S. Heise, R. Sutarto, Z. Hu, C. Chang, H. Hsieh, H.-J. Lin, C. Chen, and L. Tjeng, Phys. Rev. B **73**, 094407 (2006).
[13]R. Sutarto, S. Altendorf, B. Coloru, M. M. Sala, T. Haupricht, C. Chang, Z. Hu, C. Schüßler-Langeheine, N. Hollmann, H. Kierspel, J. Mydosh, H. Hsieh, H.-J. Lin, C. Chen, and L. Tjeng, Phys. Rev. B **80**, 085308 (2009).
[14]T. Mairoser, A. Schmehl, A. Melville, T. Heeg, L. Canella, P. Böni, W. Zander, J. Schubert, D. Shai, E. J. Monkman, K. M. Shen, D. G. Schlom, and J. Mannhart, Phys. Rev. Lett. **105**, 257206 (2010).
[15]T. Mairoser, A. Schmehl, A. Melville, T. Heeg, W. Zander, J. Schubert, D. E. Shai, E. J. Monkman, K. M. Shen, T. Z. Regier, D. G. Schlom, and J. Mannhart, Appl. Phys. Lett. **98**, 102110 (2011).

[16]K. Y. Ahn and M. W. Shafer, J. Appl. Phys. **41**, 1260–1262 (1970).
[17]K. Lee and J. C. Suits, Phys. Lett. A **34**, 141–142 (1971).
[18]Y. Capiomont, N.-V. Dang, O. Massenet, and B. K. Chakraverty, Solid State Commun. **10**, 679–683 (1972).
[19]T. R. McGuire, G. F. Petrich, B. L. Olson, V. L. Moruzzi, and K. Y. Ahn, J. Appl. Phys. **42**, 1775–1777 (1971).
[20]R. P. Ingel and D. Lewis III, J. Am. Ceram. Soc. **69**, 325–332 (1986).
[21]P. D. Dernier and R. G. Maines, Mater. Res. Bull. **6**, 433–440 (1971).
[22]R. Sutarto, S. G. Altendorf, B. Coloru, M. M. Sala, T. Haupricht, C. F. Chang, Z. Hu, C. Schüßler-Langeheine, N. Hollmann, H. Kierspel, H. H. Hsieh, H.-J. Lin, C. T. Chen, and L. H. Tjeng, Phys. Rev. B **79**, 205318 (2009).
[23]R. W. Ulbricht, A. Schmehl, T. Heeg, J. Schubert, and D. G. Schlom, Appl. Phys. Lett. **93**, 102105 (2008).
[24]V. Srivastava, S. Bhajanker, and S. P. Sanyal, Physica B **406**, 2158–2162 (2011).
[25]A. R. Kortan, M. Hong, J. Kwo, J. P. Mannaerts, and N. Kopylov, Phys. Rev. B **60**, 10913–10918 (1999).
[26]C. Kim, I. K. Robinson, T. Spila, and J. E. Greene, J. Appl. Phys. **83**, 7608–7612 (1998).
[27]P. F. Miceli and C. J. Palmstrom, Phys. Rev. B **51**, 5506–5509 (1995).
[28]R. Schiller and W. Nolting, Solid State Commun. **110**, 121–125 (1999).
[29]M. Müller, G.-X. Miao, and J. S. Moodera, J. Appl. Phys. **105**, 07C917 (2009).
[30]E. Negusse, J. Dvorak, J. S. Holroyd, M. Liberati, T. S. Santos, J. S. Moodera, E. Arenholz, and Y. U. Idzerda, J. Appl. Phys. **105**, 07C930 (2009).
[31]M. Barbagallo, T. Stollenwerk, J. Kroha, N.-J. Steinke, N. D. M. Hine, J. F. K. Cooper, C. H. W. Barnes, A. Ionescu, P. M. D. S. Monteiro, J.-Y. Kim, K. R. A. Ziebeck, C. J. Kinane, R. M. Dalgliesh, T. R. Charlton, and S. Langridge, Phys. Rev. B **84**, 075219 (2011).
[32]G. Kresse and J. Furthmüller, Phys. Rev. B **54**, 11169–11186 (1996).
[33]J. P. Perdew, K. Burke, and M. Ernzerhof, Phys. Rev. Lett. **77**, 3865–3868 (1996).
[34]E. Bousquet, N. A. Spaldin, and P. Ghosez, Phys. Rev. Lett. **104**, 037601 (2010).
[35]V. G. Tissen and E. G. Ponyatovskil, JETP Lett. **46**, 361–364 (1987).
[36]N. Souza-Neto, J. Zhao, E. Alp, G. Shen, S. Sinogeikin, G. Lapertot, and D. Haskel, Phys. Rev. Lett. **109**, 026403 (2012).
[37]C. Giacovazzo, H. L. Monaco, G. Artioli, D. Viterbo, G. Ferraric, G. Gilli, G. Zanotti, and M. Catti, *Fundamentals of Crystallography*, 2nd ed. (Oxford University Press, Oxford, 2002), p. 337.
[38]T. Mairoser, F. Loder, A. Melville, D. G. Schlom, and A. Schmehl, Phys. Rev. B. **87**, 014416 (2013).